JEE Journal of Ecological Engineering

*Journal of Ecological Engineering*, 2025, 26(8), 352–366
https://doi.org/10.12911/22998993/204120
ISSN 2299–8993, License CC-BY 4.0

Received: 2025.04.08
Accepted: 2025.05.26
Published: 2025.06.10

# Photocatalytic degradation of micro-polyvinyl chloride using green-synthesized iron nanoparticles

Teeba M. Al-Munayzil [1], Kossay K. Al-Ahmady[2], Rasha Khalid Sabri Mhemid[1]

[1] College of Environmental Sciences, University of Mosul, Mosul 41002, Iraq
[2] Ministry of Higher Education and Scientific Research, Baghdad, Iraq
* Corresponding author's email: rashamhemid@uomosul.edu.iq

## ABSTRACT

The growing concern over plastic pollution and the environmental risks associated with microplastics (MPs) has garnered significant attention. Since conventional water treatment plants are not designed to effectively capture MPs, their effluents have become a major source of aquatic contamination. This study presents an eco-friendly approach utilizing iron nanoparticles (Fe-PP NPs), synthesized through green chemistry from pomegranate peel extract, as photocatalysts for the degradation of micro-polyvinyl chloride (Micro-PVC) in aqueous solutions. The synthesized Fe-PP NPs and micro-PVC surfaces were thoroughly characterized using scanning electron microscopy (SEM) and Fourier transform infrared spectroscopy (FTIR) to examine their morphology and composition before and after photodegradation. The photocatalytic process was optimized using response surface methodology (RSM) with a central composite design (CCD) to assess key operational parameters influencing degradation efficiency. The Fe-PP NPs exhibited high photocatalytic activity, achieving 95% micro-PVC removal under optimal conditions: 50 mg/L catalyst concentration, 5 mg micro-PVC weight, pH 3, and a reaction time of 30 days. The CCD model predictions closely matched the experimental data, confirming the reliability and effectiveness of this approach. This study highlights the potential of green-synthesized Fe-PP NPs as a sustainable solution for microplastic pollution in water treatment.

**Keywords:** microplastics, micro-PVC removal, photodegradation, green synthesis, iron nanoparticles, response surface methodology.

## INTRODUCTION

Over the past few decades, the plastic industry has grown significantly. Between 1950 and 2021, world plastic production increased from 1.5 to 390.7 million tons. Plastics are appealing for extensive commercial, industrial, medicinal, and municipal applications due to their low density, durability, outstanding chemical and biological resistance, flexibility, and low cost (Al-Hussayni et al., 2023). Today's industries and societies can't live without plastic (Chattopadhyay et al., 2023; Ortiz et al., 2022a). There is a high demand for plastic products, so plastic is produced in large quantities (Ariza-Tarazona et al., 2023). The fragmentation and aging of these products can result in microplastics (MPs) with sizes between 1 μm and 5 mm, which are dangerous to aquatic ecosystems (Altaee et al., 2024; Jiehong He, 2023). Due to the small particle size of MPs, the following features make them a cause for concern: (1) they can transfer rapidly in the environment; (2) they have a large surface area for contaminants to adhere to; (3) they are easily transported and transferred in the food web; and (4) they may be transmitted to animals. Based on their sources, MPs can be divided into primary and secondary plastics. Among the forms in which primary MPs are discharged are beads, pellets, fibers, and other materials (Chattopadhyay et al., 2023). Conversely, secondary MPs are created by biological, physical, and chemical processes on bigger plastics (Nabi et al., 2021). Moreover, the presence of MPs has also been detected in almost all ecosystems, including oceans and continents, sediments, soils, and even bottled

water. Many organisms, especially aquatic ones, ingest this plastic debris once they reach the environment, resulting in their introduction into the food chain and human consumption of MPs later on (Ortiz et al., 2022b). Gomiero et al. (2021) mentioned that humans are exposed to microplastics by inhaling them in the air and drinking water that contains them. Previous study has found micro-polymers in large amounts in drinking water treatment plants (DWTP) (Mrowiec, 2018). One of these polymers is micro-PVC, which is highly resistant to conventional treatment processes. DWTPs detected higher quantities of MPs corresponding to polymers with relatively high density, like PVC. Moreover, wastewater treatment plants (WWTPs) and DWTPs face challenges in effectively removing MPs with sizes between 10 and 50 µm and nanoparticle formation during some processes (Kim et al., 2022). Piazza et al. (2022) note that PVC microplastics (PVC-MPs) negatively impact marine ecosystems and human health. methods to mitigate PVC-MPs pollution has become an urgent priority (Sultan et al., 2023). Advanced oxidation procedures (AOPs) are superior to previous artificial aging methods because they are stable and effective under a variety of conditions, and they also have fewer operating costs and complications (Su et al., 2024). Hence, this research attempts to degrade this pollutant through a photodegradation method, which is a one of advanced oxidation processes (AOPs) and analyzes the efficacy of the process through various characterization techniques. The Fenton reaction, ozonation, and electrochemical treatments are examples of AOPs that are frequently employed to break down organic pollutants in water. These procedures have recently been used for the cleanup of microplastics. Theoretically, combining photocatalysis with the Fenton reaction can increase the generation of photogenerated electrons, which swiftly move to iron and change its composition from $Fe^{3+}$ to $Fe^{2+}$. This reduction leads to charge separation and activates the Fenton process. The breakdown of organic molecules is accelerated by the regenerated $Fe^{2+}$, which encourages the quick production of hydroxyl radicals (•OH). For these applications, the photo-Fenton technique is therefore thought to be very effective, controlled, and economical. The classical homogeneous Fenton reaction has a number of drawbacks, including a low pH, the generation of large amounts of iron sludge, and the need for significant amounts of $F^{2+}$, resulting in the proposal of heterogeneous processes to overcome these limitations (Piazza et al., 2022). The chemical and physical processes used in the manufacture of catalysts cause toxic solvents, hazardous waste, and excessive energy consumption (Maurya et al., 2019). To produce environmentally friendly and sustainable nanoparticle catalysts, research and development are required. In the biosynthetic process (also called green synthesis), nanoparticles are synthesized using plants and microbes as reducing agent. Among the benefits of this technology are its non-toxicity, economic efficiency, biocompatibility, sustainability, reduced environmental impact, and ability to act as an efficient photocatalyst for pollutant degradation without producing toxic byproducts (Nabi et al., 2021).Therefore, in this work, the degradation of microplastics was performed using heterogeneous photo-Fenton reaction utilizing solid catalyst consisting $Fe_2O_3$ nanoparticles as a source of iron ions ($Fe^{2+}$), which it is extraction greenly from pomegranate peels. As far as we know, the published literature has mainly presented data on microplastic photocatalytic degradation technologies. A limited number of studies have assessed the degradation of MPs using green nanocatalysts.

The main goals of this study are as follows: (1) green synthesis fabrication of low-cost and eco-friendly iron nanoparticles using the extract of pomegranate peels; (2) investigation of the photo-degradation of MPs-PVC under solar irradiation in a batch system; (3) study the effects of various experimental parameters affecting the photocatalytic degradation, such as pH, time, catalyst loading, and catalyst type, on the micro-PVC removal in the batch system; and (4) find the optimization of process parameters using response surface methodology (RSM), where RSM is a set of mathematical and statistical techniques for analyzing data.

## EXPERIMENTAL PROCEDURE

### Materials and chemicals

PVC plastic was purchased from the Al-Azhar factory in Iraq. $C_2H_3Cl$ is the chemical formula. It has a density of 1.38 grams per cubic centimeter and a molecular weight of 62.5 grams per mole. A 30% weight-based hydrogen peroxide solution and a 0.45 m cellulose nitrate filter paper were provided by the College of Environmental

Sciences Laboratory at the University of Mosul. NaOH, 95%, hydrochloric acid, 37%, and ferrous chloride, 99.5% purity, 126.751 g/mol, were used to adjust the pH of the solutions.

## Micro-scale PVC plastic preparation

A polyvinyl chloride (PVC) plastic sample was used in this study. The PVC samples were grated into different sizes using scissors and a bastard-cut hand file to produce PVC particles. To eliminate larger debris and obtain particles within the micro-plastic scale (Alhajar et al., 2024), the plastic particles were passed through sieves measuring between (0.3 and 1) mm (Auta, 2017). A particle size range was selected based on studies examining the presence of microplastics in aquatic environments (Warrier et al., 2022; Fardami et al., 2023). The PVC particles were also sterilized by soaking them in 70% ethanol for 30 minutes, followed by rinsing them with sterile water for 20 minutes (Das and Kumar, 2015).

## Catalyst synthesis and characterization

### *Preparation of pomegranate peel (PP) extract*

In Figure 1, freshly picked pomegranate peels were collected, thoroughly clean with tap water, and rinsed with distilled water. After sun drying for three to four days, they were heated in an oven at 60 °C for 1.5 to 2.5 hours in order to completely remove all moisture. To achieve the desired consistency, the dried peels were ground using an electric grinder. 20 g of dried peel powder were heated with 300 mL of distilled water at 60 °C for 30 minutes to prepare the extract until the aqueous extract solution color started to be close to light yellow (Jain et al., 2021). Afterwards, the resulting solution was cooled to room temperature and discarded.

### *Green synthesis of Fe nanoparticles (Fe NPs) using waste pomegranate peel extract*

A mixture of yellow-colored pomegranate peel extract (in a 2:3 ratio) and 0.5 g of freshly prepared $FeCl_2$ was combined in equal proportions at room temperature. NaOH was gradually added drop by drop to adjust the pH to 6.0. As the solution was mixed, its color rapidly changed from yellow to vivid black, indicating the formation of iron nanoparticles (Fe NPs-PP). The solution was then heated on a hot plate, leading to the formation of a black solid precipitate. This precipitate was finely ground, washed with ethanol, and dried in an oven. The resulting material was subsequently used as a catalyst (Jain et al., 2021). As indicated in Figure 2.

## Analytical methods

### *Characterization methods*

A series of characterization techniques were conducted to analyze the synthesized catalyst (Fe NPs-PP) and micro-PVC before and after degradation.: A scanning electron microscope (SEM)-EDS device (ZEISS EVO-10, Germany) was used to study the morphology and particle size at Nineveh University; At Mosul University, Fourier transform infrared spectroscopy (FTIR, IRAffinity-1S, SHIMADU, Japan) was used to identify functional groups and analyze covalent bonds in the materials; The point of zero charge (PZC) of the catalyst was determined using the salt addition method (Subramanian et al., 1988) at the Environmental Technologies Laboratory, Mosul


**Figure 1.** Pomegranate peel extract


**Figure 2.** Preparation process of Fe NPS

University. This measurement was conducted to evaluate the surface charge of Fe NPs-PP during photodegradation, following the methodology described by (Subramanian et al., 1988).

### *Carbonyl index*

FTIR spectra were examined to estimate the Carbonyl Index (CI), a critical indicator of the oxidation level in PVC microplastics (Du et al., 2021). FTIR analyzes the oxidation by-products that contain carbonyl groups; In this case, the CI was calculated by taking the ratio of the carbonyl peak intensity to the reference peak intensity (AlHamedi et al., 2009). In this work, CI was used to measure the oxidation and its chemical effects on PVC.

The PVC microplastics showed the presence of the characteristic absorption peak (1710–1730 $cm^{-1}$) due to carbonyl stretching, which underwent oxidation and thus changed in intensity. The peak at 1715 $cm^{-1}$ produced a remarkably strong infrared absorption signal which is indicative of oxidation (Natarajan et al., 2011). Unfortunately, CI computation has no universally acceptable method; Some choose to compare areas of absorption to each other while others use peak height (Du et al., 2021). Reference peaks in FTIR spectra are selected based on the transmission or absorption patterns, which differ from one study to the other. In this study, the absorbance was determined from transmittance using Equation 1 to write out the peak height. The reference peak was selected based on methylene (-$CH_2$-) symmetric stretching vibration as it is more consistent and therefore more reliable for measuring CI on PVC microplastics. The CI was calculated as shown in Equation 2,

$$A = log_{10} \frac{1}{T(maximum\ heigt)} \quad (1)$$

$$A = \frac{A_{carbonyl\ group(1710-1730)}}{A\ methylene\ group\ (2910 \text{for pvc})} \quad (2)$$

## Experimental process

On clear-sky days between August and November 2024, all solar light photocatalytic degradation experiments were conducted outdoors in an open environment from mid-morning (around 10:30 am) to late afternoon (3:30 pm). Under solar radiation, the experiments were conducted in a 1000 mL batch glass reactor with a magnetic stirrer as shown in Figure 3.To minimize scattering, a mirror was located at the bottom of the reactor, and aluminum foil was applied to the outer perimeter of the reactor to act as a reflector. In order to prevent solution evaporation, the reactor was covered with a Petri dish made of

**Figure 3.** Batch system

glass. The photocatalytic degradation of micro-PVC using Fe nanoparticles (NPs) in an aqueous solution containing de-ionized water was performed at three pH levels (acidic, basic, and neutral). The initial reaction mixture in the reactor was stirred at 350 rpm for two hours in the dark to stabilize the electrostatic interactions between the microplastics and the catalyst (Dong et al., 2022). Afterward, the photoreaction was initiated under sunlight. Using Whatman 42 paper filters, microplastics were isolated from the aqueous suspension every six days following each irradiation period. According to the above procedures, microplastics were processed continuously at different times (6, 12, 18, 24 and 30 days). The reaction period was determined based on a previous study by Dos Santos et al. (2023), which reported that no toxic byproducts were detected at and beyond 30 days of treatment. After collecting the microplastics, they were thoroughly washed with deionized water to remove any residual Fe nanocatalyst. Afterwards, the microplastics were dried at room temperature for 12 hours, then at 50 °C in an oven for 2 hours. Drying the microplastics was followed by reintroducing them into fresh nanocatalyst solutions. Each experiment was duplicated to minimize errors.

The effects of different parameters were assessed by varying one variable at a time while keeping others constant, like pH, catalyst concentration, pollutant weight, and reaction time, to obtain ideal conditions. Two control experiments were conducted to evaluate the degradation process. The first control involved a blank aqueous solution maintained in the dark under identical experimental conditions. The second control was a photolysis experiment performed under the same conditions but without the addition of a catalyst to assess degradation in the absence of photocatalysis. Following the equation below (3), degradation efficiency was determined by calculating the percentage of weight loss of PVC microplastics (Chattopadhyay et al., 2023).

$$Micro-PVC degradation\ efficiency\ \% = \frac{Initial\ weight\ -Degraded\ weight}{Initial\ weight} \times 100\% \quad (3)$$

### *Statistical analysis based on the response surface methodology (RSM)*

Statistical tools such as RSM are useful for predicting and modelling interactions between independent Table 1 and dependent variables. Box-Behnken, face-centered, and central composite designs (CCD) are used to improve experimental designs. Considering its simplicity and efficiency, the CCD method was used in this study. By expanding the first-order axial and radial points, we can calculate the second-order parameters (2N) (Khoshnamvand et al., 2018). In present study, the CCD was employed to determine the optimal conditions and determine how independent factors influenced the response (micro-PVC photodegradation). According to Equation 4, the dependent and independent variables are related through a second-order polynomial analysis (Aslani et al., 2016)

$$y = bo + \sum_{i=1}^{k} biXi + \sum_{i=1}^{k} biiX_i^2 + \sum_{i=1}^{k-1} \sum_{i<j=2}^{k} bijXiXj + c \quad (4)$$

where: $Y$ is the estimated response, $bo$ is a fixed value, $bi$, $bii$, and $bij$ are regression coefficients for linear, second-order, and reacted effects; $Xi$ and $Xj$ are independent elements; $k$ is the number of independent variables ($k = 4$ in this study), and $c$ is the forecast error.

The model's reliability and validity were assessed using an Analysis of Variance (ANOVA). The number of fits, the P-value, the F-value, and the $R^2$ value were examined in order to determine lack of fit. It was considered statistically significant if the P-value was less than 0.05. Models

**Table 1.** Independent factors and their intervals

| Independent variables | Symbol | Units | Level and range (coded) -1 | 1 |
|---|---|---|---|---|
| Catalyst Fe-PP nanocomposites conc. | A | mg/L | 25 | 100 |
| Micro-PVC conc. | B | mg | 5 | 20 |
| pH | C | | 3 | 11 |
| Time | D | day | 6 | 30 |

with an $R^2$ value close to 1 are considered highly accurate, whereas models with a lower $R^2$ value are considered less reliable (Sulaiman and Alwared, 2022).

## RESULTS AND DISCUSSIONS

### Scanning electron microscopy

#### *SEM analysis of Micro-PVC*

Surface morphology changes in PVC microparticles were assessed using scanning electron microscopy (SEM). Initially, the pristine micro-PVC surface, shown in Figure 4a, was smooth and flat. However, after 30 days of photodegradation treatment with 5 mg and 50 mg of NPS at pH 3 under solar radiation Figure 4b, various holes and cracks emerged. Additionally, surface fragments appeared ready to peel off due to ongoing free radical attack. It can be assumed that the peeling of these fragments contributes to the formation and expansion of holes and cracks on the surface (Ariza-Tarazona et al., 2023; Horne, 2020). In the control groups, no change was observed when they were kept in the dark. Generally, MPs exhibited greater surface changes in the presence of NPS, suggesting that NPS promoted the photodegradation of MPs. The chromophores of PVC microplastics react with UV, resulting in the ageing of their surfaces (Lin, 2020). Dong et al., (2022) found that direct photolysis prevails at low oxidant levels or early stages, while higher oxidant concentrations shift the process toward indirect photolysis, such as the photocatalysis process.

#### *SEM of NPs Fe-PP*

The SEM analysis of Fe NPs-PP in Figure 5a. reveals that the nanoparticles aggregate, resulting in unevenly shaped surface particles with rough textures. This aggregation occurs due to the magnetic properties of iron nanoparticles (Feng and Lim, 2007). The aggregates also contribute to increased porosity of the NPs Fe-PP photocatalyst. There is a possibility that this shape is caused by polyphenols in the fruit extract, which are known to affect iron nanoparticles' final morphology and size (Wu et al., 2015). After processing, the SEM

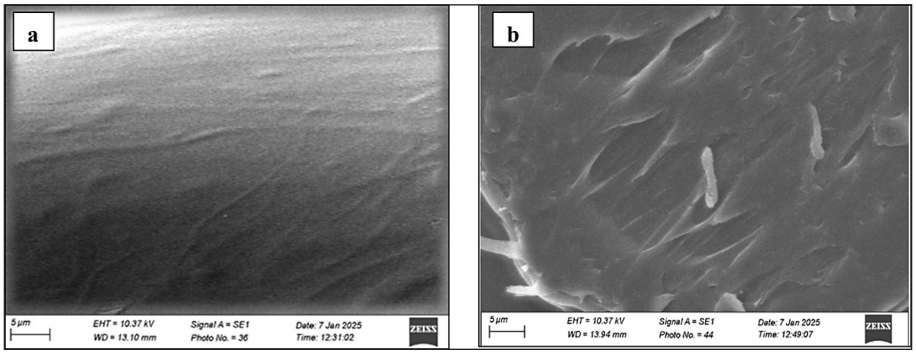


**Figure 4.** SEM images showing the photodegradation process of micro-pvc: (a) before treatment, (b) after treatment

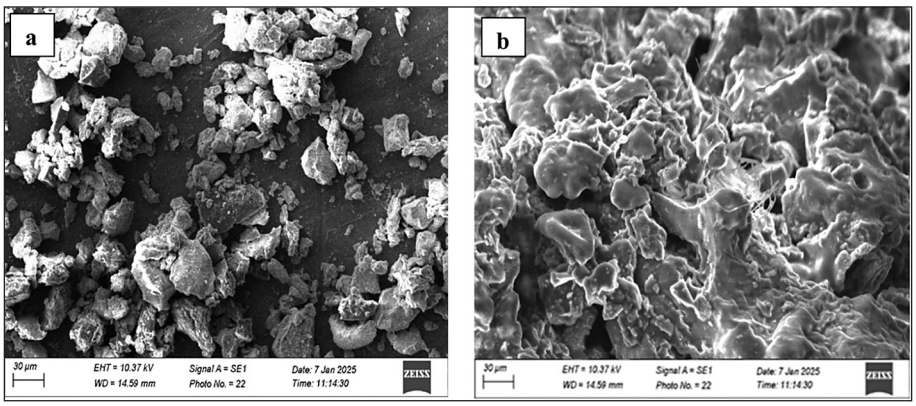


**Figure 5.** SEM images of Fe NPs-PP: (a) before treatment, (b) after treatment

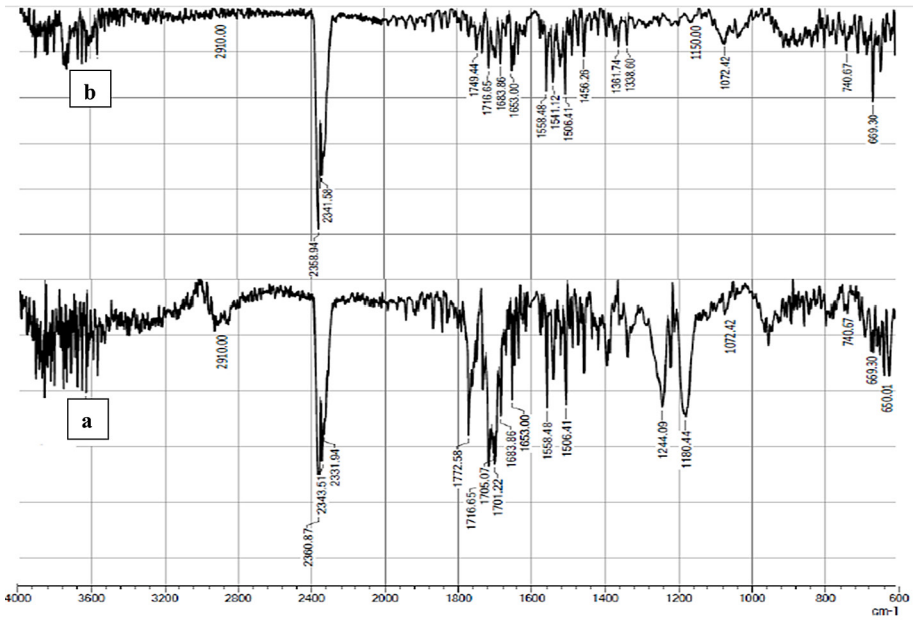


**Figure 6.** FTIR of Micro-PVC: (a**)** before, (b**)** after photodegradation

images in Figure 5b. depicted that the synthesized Fe NPs-PP are porous and spherical, with varying diameters. This nanoparticle structure enhances micro-PVC removal due to improved catalytic activity. The size variation of the nanoparticles is attributed to differences in the local concentration of pomegranate peel extract involved in metal ion reduction (Luaibi, 2022)

## FTIR analysis

### *FTIR analysis of Micro-PVC*

Figure 6 illustrates the changes in the surface functional groups of micro-PVC after being exposed to sunlight under specific conditions: an initial nanoparticle (NPs) Fe-pp dosage of 50 mM, 5 mg of micro-PVC, a pH of 3, and an irradiation period of 30 days. The infrared spectrum of micro-PVC, as shown in Figure 6a., displays two distinct peaks related to chlorine. These peaks, located at 650 $cm^{-1}$, 1244.09 $cm^{-1}$, and 1180.44 $cm^{-1}$, are attributed to C-H bending vibrations from the C-Cl and CH-Cl groups in micro-PVC (Jiang et al., 2022). Additionally, a peak at 2910 $cm^{-1}$ corresponds to the stretching vibration of the -$CH_2$ group. It can be clearly observed that the signal intensity 1716 $cm^{-1}$ belonging to the C=O group is the strongest (Park et al., 2018). The functional groups of micro-PVC after irradiation were very noticeable compared to those obtained before irradiation. Figure 6b, for micro-PVC after irradiation the intensity change in functional groups at 1705.07, 1701.22, 1653, 1683.86 $cm^{-1}$ of (C=O) and 1558.48 $cm^{-1}$ (C=C) were checked, which increased remarkably after exposure to sun irradiation (Miao et al., 2020). The intensity of signal at 2910 $cm^{-1}$ decreased. However, the characteristic peak signals of CH-Cl and C-Cl groups related to chlorine both showed different degrees of enhancement after treatment, which may be related to the inability of oxidizing radicals to attack the C-CI bond directly. In conclusion, the enhancement of the signals at 669.3, 740.67 and 1072.42 $cm^{-1}$ illustrates the inability of oxidizing radicals to release $Cl^-$ by selectively breaking the C-Cl bond. A new characteristic peak at 1150 $cm^{-1}$ emerged the spectrum of micro-PVC treated with in polymer backbone, attributable to the C-O group. This may be because in the early stage of ageing, the plasticizer is released from MPs, and in the later stage, oxygen-related functional groups are formed on the surface of the plastic (Shi et al., 2021). Furthermore, the peak in tensity at 3100 $cm^{-1}$ decreased after solar exposure that is an indicative of the loss of alkene, suggesting the scission of polymeric chains of micro-PVC. In deed the disappear in ketone (1772.58 $cm^{-1}$), C=O (1705.07 $cm^{-1}$), Alkylketone (1244.09 $cm^{-1}$) and 1180.44 $cm^{-1}$ carbonyl compound.

### *FTIR of NPs Fe-PP*

FTIR analysis for Fe NPs-PP was performed. Numerous peaks were found in the (1000–4000 $cm^{-1}$) range. As shown in Figure 7a., A large

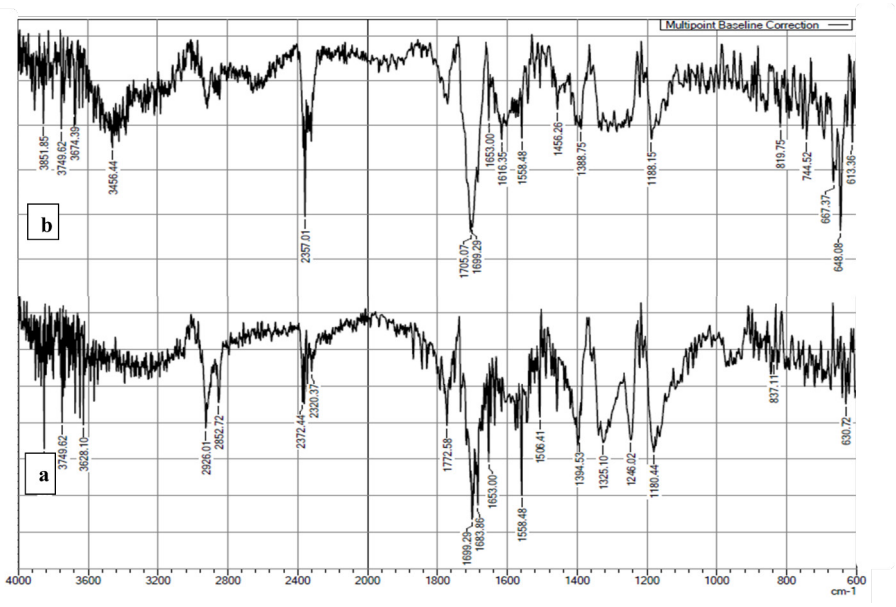


**Figure 7.** FTIR of NPs Fe-PP: (a**)** before, (b**)** after photodegradation

absorption band between (3850 and 3000 $cm^{-1}$) in the FTIR before and after spectrum was found, and it is known to be caused by the O-H stretching vibrations of H-bonded polyphenols(Wang et al., 2015). These polyphenols decrease Fe(II) ions due to their potent antioxidant properties, which causes them to adsorb on the surface of iron nanoparticles subsequently (Eslami et al., 2018). This will increase the layer life of the iron NPs by providing a layer cover to shield them from ambient oxygen. Moreover, the vibrations of the $CH_2$, C-O, alkenyl C=C, and C-O-C stretching bands at 1558.48, 1180.44, 1653.00, and 1282.02 $cm^{-1}$ are all indicative of water-soluble phytochemicals(Farahmandjou and Soflaee, 2015).Hence, the spectral analysis revealed that the polyphenols are attached to the surface of these particles and make up a crucial part of iron nanoparticles. Also, the creation of $Fe_2O_3$ at the surface of NPs Fe -PP is confirmed by a strong bonding between 600 and 700 $cm^{-1}$ caused by Fe-O stretching vibrations, which is consistent with the finding (Chakraborty et al., 2024; Mohammed et al., 2023). On the other hand, in Figure 7b. the bands at 2926.01 $cm^{-1}$ and 2852.72 $cm^{-1}$ which correspond to C-H bonds are completely inhibited compared to the raw nanoparticles. Peak changing in intensities could possibly be due to the presence of active adsorptive sites(Mohammed et al., 2023). CI (carbonyl index) measures the ageing of microplastics (MPs) during oxidation, reflecting changes in their properties during oxidation (Domínguez-Jaimes et al., 2021).According to Table 2, there was an increase in CI values after photodegradation, suggesting the formation of oxygen-containing functional groups during photodegradation. Notably, CI values were highest at pH 3 (4.06) compared to pH 11 (3.958), pH 7 (2.279), and the original micro-PVC (2.49). Photo-oxidation of hydrocarbons generates carbonyl groups as the degradation process progresses, increasing the CI values after degradation. Therefore, higher CI values should be expected after a photodegradation process (Ariza-Tarazona et al., 2023; Su et al., 2024).

## Zero potential charge of $Fe_2O_3$-PP

To determine the charge on the Fe NPs-PP surface during photodegradation, the point of zero charge ($pH_{ZPC}$) must be identified. As shown in Figure 8, the $pH_{ZPC}$ at the point of intersection for Fe NPs-PP is 7.5. Increasing solution pH leads to a decrease in positive charges on the catalyst surface. Thus, when the pH is below the pHpzc, the surface charge is positive and negative when

**Table 2.** CI values of origin and treated PVC

| Sample | CI (A1716/A2910) |
|---|---|
| PVC -original | 2.49 |
| PVC-PH3 | 4.06 |
| PVC-PH11 | 3.958 |
| PVC-PH7 | 2.279 |

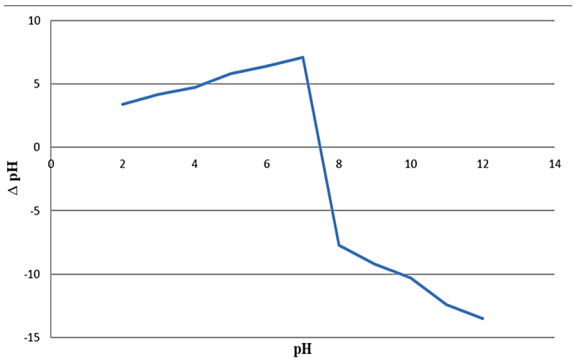


**Figure 8.** The zero-potential charge of FeNPS -PP at different PHs values

the pH is above this point (Sun et al., 2012). This suggests that the adsorption-desorption characteristics of the chemicals are highly sensitive to pH changes (Azeez et al., 2018).

## Photocatalytic activity of batch experimental results

### *RSM analysis of micro-PVC photodegradation*

In this study, 35 tests were conducted using Design-Expert software (version 13) to evaluate NPS-Fe-PP's effectiveness at removing PVC microplastics (MPs). The objective of this study was to determine the most efficient removal rate. Micro-PVC removal efficiency was correlated with pH, catalyst dosage, reaction time, and initial microplastic weights. In Table 3, the results show that NPS-Fe-PP showed a wide range of effectiveness, ranging from 1.42% to 95.48 %.

Analysis of variance (ANOVA) as detailed in next section was used to examine the quadratic model in Equation (5), which includes input variables (A, B, C, D) and their quadratic terms ($A^2$, $C^2$, $D^2$) affecting the response variable (Y). Positive coefficients indicate direct correlations, while negative ones indicate inverse relationships. An ANOVA analysis reveals the model's significance and the contributions of individual terms.

The impact coefficients for micro-PVC degradation using Fe NPs-PP under solar light are ranked as follows: D > $C^2$ > A > $A^2$ > $D^2$ > CD > B > C. The photocatalytic removal efficiency can be predicted using Equation (1) within the specified experimental ranges.

$$\begin{aligned} \textit{Micro-PVC removal}\ (Y) = {} & 43.13104 + \\ & + (1.07812 \times A) + (-1.278 \times B) + \\ & + (-25.7033 \times C) + (3.81857 \times D) + \\ & + (-0.098178 \times C \times D) + (-0.007455 \times A^2) + \\ & + (1.86575 \times C^2) + (-0.024371 \times D^2) \end{aligned} \quad (5)$$

### *ANOVA and regression analyses for micro-PVC removal*

Table 4 results show a satisfactory fit, with an $R^2$ difference of < 0.2 (expected $R^2$: 0.9644, adjusted $R^2$: 0.9803). ANOVA confirms the significance of the quadratic response surface model (Azzaz et al., 2021). ANOVA Analysis (Table 5) shows that four single-effect terms (A, B, C, D), the interaction term (CD), and three quadratic terms ($A^2$, $C^2$, $D^2$) are statistically significant (P < 0.05). The Model F-value of 213.01 and corresponding p-value < 0.05 confirm model significance, with only a 0.01% chance of this F-value arising from noise. Terms with p-values > 0.05 were excluded to refine the microplastic removal model (Manjunath et al., 2017).

### *Evaluation of effective parameter interactions and determination of optimal conditions*

In these experiments, a single process variable (pH, MP weight, catalyst concentration, or reaction time) was varied at a time while keeping the others constant to evaluate their interactions. The objective was to gain a deeper understanding of their impact on removal efficiency. Figure 9 (a–c) present three-dimensional surface plots illustrating MP removal using nanoparticles. After 2 hours of mixing in the dark, the reactants were exposed to sunlight to achieve adsorption/desorption equilibrium. Afterwards, the solar photocatalytic degradation process of PVC-MPs was initiated.

In this study, initial pH levels of 3, 7, and 11 were evaluated under fixed conditions (Fe photocatalyst at 50 mg/L, MP mass at 5 mg, and reaction times of 6–30 days (Table 3). Maximum micro-PVC removal occurs at pH 3, as the negatively charged PVC surface (Cai et al., 2020) is strongly attracted to the positively charged of catalyst surface below the point of zero charge ($pH_{Z\text{-}PC}$), enhancing oxidation efficiency. At this pH, the photocatalytic activity of $Fe_2O_3$ nanoparticles reached 95.48% Figure 9a. These findings suggest that pollutant charge neutralization is significantly influenced by pH, with acidic conditions (pH 3) exhibiting higher efficiency than alkaline (pH > 7) or neutral (pH 7) (Dos Santos et al., 2023). Shi et al. (2021) reported that the photodegradation efficiency of MPs was optimal at pH 3 compared to pH 7 and pH 11. Higher pH values assisted the formation of hydroperoxide radicals, further boosting MP degradation.

**Table 3.** The results and variables of the experiments related to the removal of micro-PVC using NPS-Fe-PP under sunlight

| Experiments | Factor1: A: catalyst Dose. (mg/L) | Factor2: B: MPs weight (mg) | Factor3: C: pH | Factor4: D: Time | Response: Y= micro-PVC RE% | |
|---|---|---|---|---|---|---|
| | | | | | Actual value | Predicted value |
| 1 | 3 | 25 | 5 | 6 | 18.98 | 17.45 |
| 2 | 3 | 25 | 5 | 12 | 37.50 | 37.6 |
| 3 | 3 | 25 | 5 | 18 | 54.25 | 55.13 |
| 4 | 3 | 25 | 5 | 24 | 69.26 | 70.02 |
| 5 | 3 | 25 | 5 | 30 | 82.50 | 82.29 |
| 6 | 3 | 50 | 5 | 6 | 31.96 | 30.42 |
| 7 | 3 | 50 | 5 | 12 | 50.47 | 50.58 |
| 8 | 3 | 50 | 5 | 18 | 67.23 | 68.1 |
| 9 | 3 | 50 | 5 | 24 | 82.23 | 83 |
| 10 | 3 | 50 | 5 | 30 | 95.48 | 95.26 |
| 11 | 3 | 100 | 5 | 6 | 29.95 | 28.41 |
| 12 | 3 | 100 | 5 | 12 | 48.46 | 48.57 |
| 13 | 3 | 100 | 5 | 18 | 65.22 | 66.09 |
| 14 | 3 | 100 | 5 | 24 | 80.22 | 80.99 |
| 15 | 3 | 100 | 5 | 30 | 93.47 | 93.25 |
| 16 | 11 | 50 | 5 | 6 | 30.58 | 26.41 |
| 17 | 11 | 50 | 5 | 12 | 44.38 | 43.17 |
| 18 | 11 | 50 | 5 | 18 | 56.43 | 57.3 |
| 19 | 11 | 50 | 5 | 24 | 66.72 | 68.8 |
| 20 | 11 | 50 | 5 | 30 | 75.25 | 77.68 |
| 21 | 7 | 50 | 5 | 6 | 1.42 | 15.72 |
| 22 | 7 | 50 | 5 | 12 | 17.57 | 12.73 |
| 23 | 7 | 50 | 5 | 18 | 31.97 | 28.56 |
| 24 | 7 | 50 | 5 | 24 | 44.62 | 41.76 |
| 25 | 7 | 50 | 5 | 30 | 55.51 | 52.33 |
| 26 | 3 | 50 | 10 | 6 | 25.57 | 24.03 |
| 27 | 3 | 50 | 10 | 12 | 44.08 | 44.19 |
| 28 | 3 | 50 | 10 | 18 | 60.84 | 61.71 |
| 29 | 3 | 50 | 10 | 24 | 75.84 | 76.61 |
| 30 | 3 | 50 | 10 | 30 | 89.09 | 88.87 |
| 31 | 3 | 50 | 20 | 6 | 12.79 | 11.25 |
| 32 | 3 | 50 | 20 | 12 | 31.30 | 31.41 |
| 33 | 3 | 50 | 20 | 18 | 48.06 | 48.93 |
| 34 | 3 | 50 | 20 | 24 | 63.06 | 63.83 |
| 35 | 3 | 50 | 20 | 30 | 76.31 | 76.09 |

A Fe NPS catalyst concentration of 50 mg/L, a micro-PVC mass of 5 mg, a pH value of 3, and a reaction period of 30 days were ideal for achieving a maximum 95.48% removal efficiency (Figure 9b, Table 3). The results and variables of the experiments related to the removal of micro-PVC using NPS-Fe-PP under sunlight:, E (1–15). When the catalyst concentration exceeded 50 mg/L, particle agglomeration occurred, reducing light transmission and thereby decreasing removal efficiency (Shihab et al., 2024). Several studies

**Table 4.** Fit statistics results for the response quadratic models

| Factors | Fit statistics results |
|---|---|
| Standard deviation | 3.43 |
| Mean | 53.10 |
| Coefficient of variance (CV, %) | 6.47 |
| Coefficient of determination ($R^2$) | 0.9850 |
| Adjusted $R^2$ | 0.9803 |
| Predicted $R^2$ | 0.9644 |
| Adequate precision | 54.0030 |

**Table 5.** ANOVA for micro-PVC by Fe NPs- pp reduced quadratic model

| Source | Sum of squares | df | Mean square | F-value | p-value | |
|---|---|---|---|---|---|---|
| Model | 20104.24 | 8 | 2513.03 | 213.01 | < 0.0001 | significant |
| A - $Fe_2O_3$ dose | 300.52 | 1 | 300.52 | 25.47 | < 0.0001 | significant |
| B - PVC-MPs. conc. | 952.75 | 1 | 952.75 | 80.76 | < 0.0001 | significant |
| C - pH | 340.20 | 1 | 340.20 | 28.84 | < 0.0001 | significant |
| D - time | 7925.42 | 1 | 7925.42 | 671.77 | < 0.0001 | significant |
| CD | 206.22 | 1 | 206.22 | 17.48 | 0.0003 | significant |
| $A^2$ | 341.97 | 1 | 341.97 | 28.99 | < 0.0001 | significant |
| $C^2$ | 3119.00 | 1 | 3119.00 | 264.37 | < 0.0001 | significant |
| $D^2$ | 75.43 | 1 | 75.43 | 6.39 | 0.0179 | |
| Residual | 306.74 | 26 | 11.80 | | | |
| Cor total | 20410.98 | 34 | | | | |

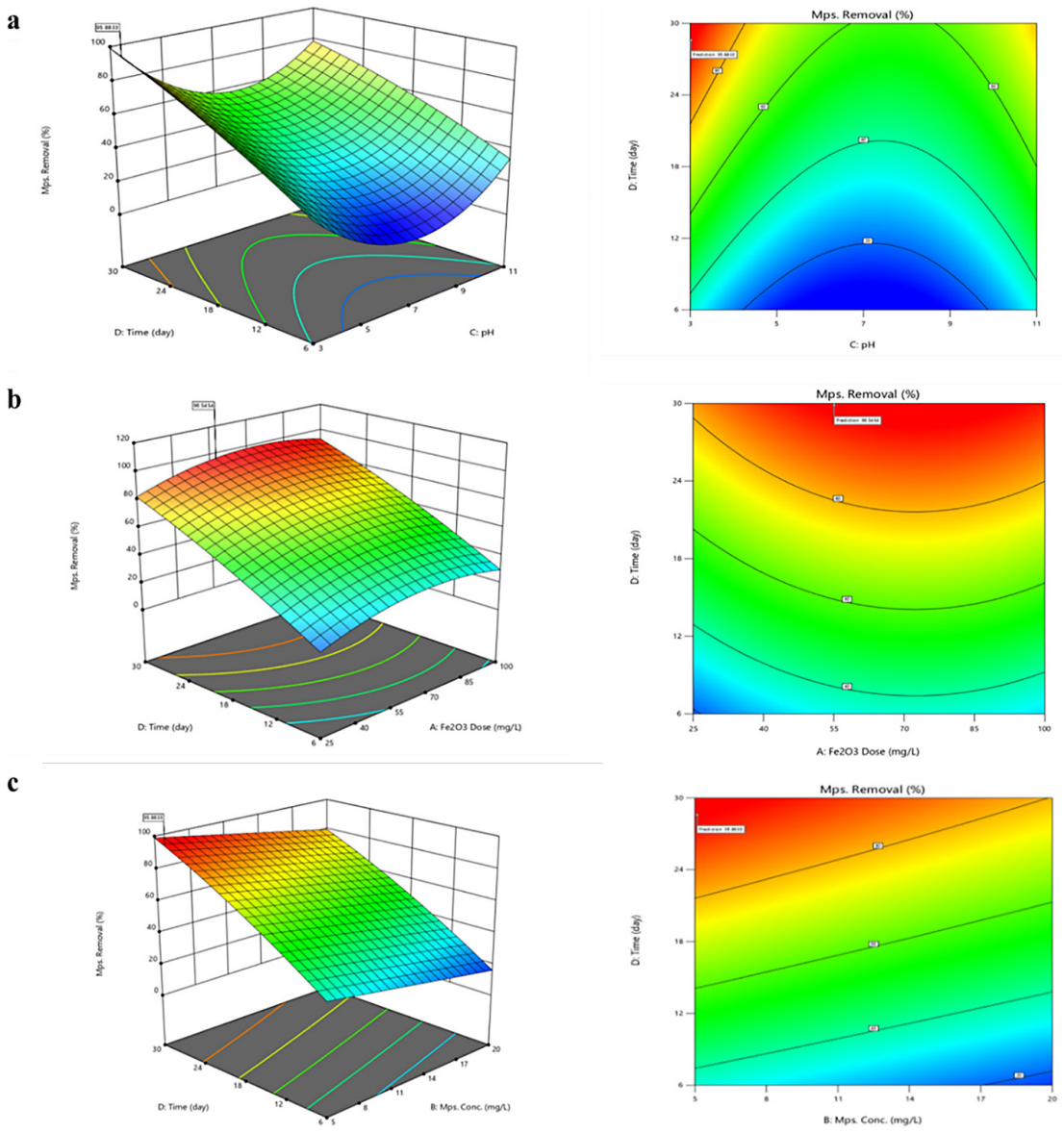


**Figure 9.** Illustrates the effects of key parameter interactions on micro-PVC removal using FeNPS-PP under solar irradiation: a) Ph versus reaction time, b) catalyst concentration versus reaction time, c) PVCMPs weight versus reaction time

have demonstrated that the semiconductors in the nanoscale enhance the interaction between the catalyst and MPs under irradiation exposure, improving the degradation process (Nabi et al., 2021; Tofa et al., 2019b).

Figure 9c illustrates the impact of micro-PVC mass and reaction time on MPs degradation using Fe-PP nanoparticles at pH 3 and 50 mg/L catalyst. Higher initial PVC-MPs weights reduced degradation rates, while longer reaction times improved removal efficiency, likely due to increased free radical formation (Mhemid et al., 2024). Thus, the highest removal efficiency was achieved at 5 mg micro-PVC and 30 days, aligning with previous studies showing a direct correlation between photocatalysis duration and microplastic weight (Jeyavani et al., 2024).

The dark control groups showed no weight loss, regardless of Fe NP addition. Similarly, in the photolysis control test without a catalyst, less than 2% of the original weight was lost, confirming negligible MP degradation.

## CONCLUSIONS

In conclusion, this study demonstrates the potential of green-synthesized iron nanoparticles (Fe-PP NPs) as an effective and eco-friendly solution for the degradation of microplastic pollution, particularly micro-polyvinyl chloride (Micro-PVC) in aquatic environments. The high photocatalytic activity of Fe-PP NPs, coupled with the optimization of key operational parameters through RSM, achieved a significant 95% removal of Micro-PVC under optimal conditions, which included a PVC weight of 5 mg, catalyst concentration of 50 mg/L, pH 3, and a reaction time of 30 days. The predicted values from the Central Composite Design (CCD) model showed reasonable agreement with the experimental data. The results of ANOVA indicated that the second-order regression model successfully fitted the experimental data ($R^2$ = 98.5%, $R^2$adj = 98.03%, $R^2$pred = 96.4%). Based on the results, it is recommended to integrate photodegradation treatment with existing DWTPS and WWTPS facilities to enhance microplastic removal efficiency in real-world applications. This approach addresses the limitations of conventional treatment plants in capturing microplastics and offers a sustainable, green chemistry-based alternative for mitigating microplastic contamination.

## Acknowledgment

The authors sincerely thank the Environmental sciences Laboratory of the University of Mosul for supporting the research by providing essential facilities.

## REFERENCES

1. Alhajar, M. W., Al-Ahmady, K. K., Khalid, R., Mhemid, S. (2024). Biodegradation of micro-polyvinyl chloride in aqueous solution. *Journal of Al-Rafidain Environment*.
2. AlHamedi, F. H., Rauf, M. A., Ashraf, S. S. (2009). Degradation studies of Rhodamine B in the presence of UV/H2O2. *Desalination*, *239*(1), 159–166. https://doi.org/https://doi.org/10.1016/j.desal.2008.03.016
3. Al-Hussayni, R. S., Al-Ahmady, K. K., Mhemid, R. K. S. (2023). Assessment of indoor air pollution by suspended micro plastic in selected sites of Mosul city. *College of Basic Education Researchers Journal*, *19*(4), 833–851.
4. Altaee, R. N., Al-Ahmady, K. K., Mhemid, R. K. S. (2024). Study the effectiveness of household water filtration systems in eliminating plastic particles in Mosul City, Iraq. *Journal of Ecological Engineering*, *25*(9), 24–33. https://doi.org/10.12911/22998993/190106
5. Ariza-Tarazona, M. C., Siligardi, C., Carreón-López, H. A., Valdéz-Cerda, J. E., Pozzi, P., Kaushik, G., Villarreal-Chiu, J. F., Cedillo-González, E. I. (2023). Low environmental impact remediation of microplastics: Visible-light photocatalytic degradation of PET microplastics using bio-inspired C,N-TiO2/SiO2 photocatalysts. *Marine Pollution Bulletin*, *193*, 115206. https://doi.org/10.1016/j.marpolbul.2023.115206
6. Aslani, H., Nabizadeh, R., Nasseri, S., Mesdaghinia, A., Alimohammadi, M., Mahvi, A. H., Rastkari, N., & Nazmara, S. (2016). Application of response surface methodology for modeling and optimization of trichloroacetic acid and turbidity removal using potassium ferrate(VI). *Desalination and Water Treatment*, *57*(52), 25317–25328. https://doi.org/https://doi.org/10.1080/19443994.2016.1147380
7. Auta H.S., Emenike C.U/, Fauziah S/H/ (2017). Screening of Bacillus strains isolated from mangrove ecosystems in Peninsular Malaysia for microplastic degradation. *Environmental Pollution*, 231(2), 1552-1559. https://doi.org/10.1016/j.envpol.2017.09.043.
8. Azeez, F., Al-Hetlani, E., Arafa, M., Abdelmonem, Y., Nazeer, A. A., Amin, M. O., Madkour, M. (2018). The effect of surface charge on photocatalytic

degradation of methylene blue dye using chargeable titania nanoparticles. *Scientific Reports*, *8*(1), 7104. https://doi.org/10.1038/s41598-018-25673-5

9. Azzaz, A. A., Jellali, S., Hamed, N. B. H., El Jery, A., Khezami, L., Assadi, A. A., Amrane, A. (2021). Photocatalytic treatment of wastewater containing simultaneous organic and inorganic pollution: Competition and operating parameters effects. *Catalysts*, *11*(7). https://doi.org/10.3390/catal11070855
10. Cai, H., Wang, Y., Wu, K., Guo, W. (2020). Enhanced hydrophilic and electrophilic properties of polyvinyl chloride (PVC) biofilm Carrier. *Polymers*, *12*(6), 1240. https://doi.org/10.3390/polym12061240
11. Chakraborty, A. R., Zohora Toma, F. T., Alam, K., Yousuf, S. B., Hossain, K. S. (2024). Influence of annealing temperature on $Fe_2O_3$ nanoparticles: Synthesis optimization and structural, optical, morphological, and magnetic properties characterization for advanced technological applications. *Heliyon*, *10*(21), e40000. https://doi.org/https://doi.org/10.1016/j.heliyon.2024.e40000
12. Chattopadhyay, P., Camila Ariza-Tarazona, M., Iveth Cedillo-González, E., Siligardi, C., Simmchen, J. (2023). *Photocatalytic collection and degradation of microplastics by self-asymmetric Pac-Man TiO2*.
13. Das, M. P., Kumar, S. (2015). An approach to low-density polyethylene biodegradation by Bacillus amyloliquefaciens. *3 Biotech*, *5*(1), 81–86. https://doi.org/10.1007/s13205-014-0205-1
14. Domínguez-Jaimes, L. P., Cedillo-González, E. I., Luévano-Hipólito, E., Acuña-Bedoya, J. D., Hernández-López, J. M. (2021). Degradation of primary nanoplastics by photocatalysis using different anodized TiO2 structures. *Journal of Hazardous Materials*, *413*, 125452. https://doi.org/10.1016/j.jhazmat.2021.125452
15. Dong, S., Yan, X., Yue, Y., Li, W., Luo, W., Wang, Y., Sun, J., Li, Y., Liu, M., Fan, M. (2022). $H_2O_2$ concentration influenced the photoaging mechanism and kinetics of polystyrene microplastic under UV irradiation: Direct and indirect photolysis. *Journal of Cleaner Production*, *380*, 135046. https://doi.org/https://doi.org/10.1016/j.jclepro.2022.135046
16. Dos Santos, N. de O., Busquets, R., Campos, L. C. (2023). Insights into the removal of microplastics and microfibres by advanced oxidation processes. *Science of The Total Environment*, *861*, 160665. https://doi.org/10.1016/j.scitotenv.2022.160665
17. Du, H., Xie, Y., Wang, J. (2021). Microplastic degradation methods and corresponding degradation mechanism: Research status and future perspectives. *Journal of Hazardous Materials*, *418*, 126377. https://doi.org/https://doi.org/10.1016/j.jhazmat.2021.126377
18. Eslami, S., Ebrahimzadeh, M. A., Biparva, P. (2018). Green synthesis of safe zero valent iron nanoparticles by: Myrtus communis leaf extract as an effective agent for reducing excessive iron in iron-overloaded mice, a thalassemia model. *RSC Advances*, *8*(46), 26144–26155. https://doi.org/10.1039/c8ra04451a
19. Farahmandjou, M., Soflaee, F. (2015). Synthesis and characterization of α-$Fe_2O_3$ nanoparticles by simple co-precipitation method. *Physical Chemistry Research*, *3*(3), 191–196. https://doi.org/10.22036/pcr.2015.9193
20. Fardami Y., A., Magami, I. M., Yarima, A. A., Sabitu, M. (2023). Microbes associated with bioremediation of microplastic waste in Nigerian freshwater bodies: a review. *UMYU Scientifica*, *2*(1), 140–150. https://doi.org/10.56919/usci.2123.017
21. Feng, J., Lim, T.-T. (2007). Iron-mediated reduction rates and pathways of halogenated methanes with nanoscale Pd/Fe: Analysis of linear free energy relationship. *Chemosphere*, *66*(9), 1765–1774. https://doi.org/https://doi.org/10.1016/j.chemosphere.2006.06.068
22. Fiona J. Horne, J. J. (2020). Photo-oxidation of poly(ethylene terephthalate) films intended for photovoltaic backsheet. *Journal of Applied Polymer Science*.
23. Gomiero, A., Øysæd, K. B., Palmas, L., Skogerbø, G. (2021). Application of GCMS-pyrolysis to estimate the levels of microplastics in a drinking water supply system. *Journal of Hazardous Materials*, *416*. https://doi.org/10.1016/j.jhazmat.2021.125708
24. Sultan, M.H., Al-Ahmady, K.K., Khalid, R., Mhemid, S. (2023). Assessment of microplastic particles in tap water on the right side of Mosul City, Iraq. *Al-Rafidain Engineering Journal* 28(2).
25. Jain, R., Mendiratta, S., Kumar, L., Srivastava, A. (2021). Green synthesis of iron nanoparticles using Artocarpus heterophyllus peel extract and their application as a heterogeneous Fenton-like catalyst for the degradation of Fuchsin Basic dye. *Current Research in Green and Sustainable Chemistry*, *4*, 100086. https://doi.org/10.1016/j.crgsc.2021.100086
26. Jeyavani, J., Al-Ghanim, K. A., Govindarajan, M., Malafaia, G., Vaseeharan, B. (2024). A convenient strategy for mitigating microplastics in wastewater treatment using natural light and ZnO nanoparticles as photocatalysts: A mechanistic study. *Journal of Contaminant Hydrology*, *267*, 104436. https://doi.org/https://doi.org/10.1016/j.jconhyd.2024.104436
27. Jiang, C., Ni, B.-J., Zheng, X., Lu, B., Chen, Z., Gao, Y., Zhang, Y., Zhang, S., Luo, G. (2022). The changes of microplastics' behavior in adsorption and anaerobic digestion of waste activated sludge induced by hydrothermal pretreatment. *Water Research*, *221*, 118744. https://doi.org/https://doi.org/10.1016/j.watres.2022.118744

28. Jiehong He, Lanfang Han, Weiwei Ma, Liying Chen, Chuanxin Ma,· Chao Xu,· Zhifeng Yang (2023). Efficient photodegradation of polystyrene microplastics integrated with hydrogen evolution: Uncovering degradation pathways. *iScience, 26*(6), 106833. https://doi.org/10.1016/j.isci.2023.106833
29. Khoshnamvand, N., Kord Mostafapour, F., Mohammadi, A., Faraji, M. (2018). Response surface methodology (RSM) modeling to improve removal of ciprofloxacin from aqueous solutions in photocatalytic process using copper oxide nanoparticles (CuO/UV). *AMB Express*, *8*(1). https://doi.org/10.1186/s13568-018-0579-2
30. Kim, S., Sin, A., Nam, H., Park, Y., Lee, H., Han, C. (2022). Advanced oxidation processes for microplastics degradation: A recent trend. *Chemical Engineering Journal Advances*, *9*. https://doi.org/10.1016/j.ceja.2021.100213
31. Jialing Lin, Deyi Yan, Jianwei Fu, Yuheng Chen, Huase Ou (2020). Ultraviolet-C and vacuum ultraviolet inducing surface degradation of microplastics. *Water*, 186, 116360. https://doi.org/10.1016/j.watres.2020.116360.
32. Luaibi, I.M., Atiya M.A., Hassan A.K., Mahmoud Z.A. (2022). Heterogeneous catalytic degradation of dye by Fenton-like oxidation over a continuous system based on Box–Behnken design and traditional batch experiments. *Karbala International Journal of Modern Science*, *8*(2), 9–28.
33. Manjunath, G. B., Bharath, K. N., Ganesh, D. B., Raj Kumar, D. G., Shivprakash, P., Harsha, H. M. (2017). ANOVA and Response Surface Methodology for the Optimization of Fracture Toughness parameters on Jute Fabric-Epoxy composites using SENB specimens. *Materials Today: Proceedings*, *4*(10), 11285–11291. https://doi.org/10.1016/j.matpr.2017.09.052
34. Maurya, I. C., Singh, S., Senapati, S., Srivastava, P., Bahadur, L. (2019). Green synthesis of $TiO_2$ nanoparticles using Bixa orellana seed extract and its application for solar cells. *Solar Energy*, *194*, 952–958. https://doi.org/https://doi.org/10.1016/j.solener.2019.10.090
35. Mhemid, R. K. S., Saeed, L. I., Mohammed, R. N. (2024). Photocatalytic removal of diazinon with Ag-coated $SiO_2$@$TiO_2$ core–shell using the response surface methodology. *International Journal of Environmental Science and Technology*, *21*(1), 329–340. https://doi.org/10.1007/s13762-023-05134-x
36. Miao, F., Liu, Y., Gao, M., Yu, X., Xiao, P., Wang, M., Wang, S., Wang, X. (2020). Degradation of polyvinyl chloride microplastics via an electro-Fenton-like system with a $TiO_2$/graphite cathode. *Journal of Hazardous Materials*, *399*, 123023. https://doi.org/https://doi.org/10.1016/j.jhazmat.2020.123023
37. Mohammed, N. A., Saeed, L. I., Mhemid, R. K. S. (2023). Sustainable production of an iron-eggshell nanocomposite and investigating its catalytic potential for phenol removal. *Ecological Chemistry and Engineering S*, *30*(3), 387–403. https://doi.org/10.2478/eces-2023-0040
38. Mrowiec, B. (2018). The role of wastewater treatment plants in surface water contamination by plastic pollutants. *E3S Web of Conferences*, *45*, 00054. https://doi.org/10.1051/e3sconf/20184500054
39. Nabi, I., Bacha, A.-U.-R., Ahmad, F., Zhang, L. (2021). Application of titanium dioxide for the photocatalytic degradation of macro- and micro-plastics: A review. *Journal of Environmental Chemical Engineering*, *9*(5), 105964. https://doi.org/https://doi.org/10.1016/j.jece.2021.105964
40. Natarajan, T. S., Thomas, M., Natarajan, K., Bajaj, H. C., Tayade, R. J. (2011). Study on UV-LED/$TiO_2$ process for degradation of Rhodamine B dye. *Chemical Engineering Journal*, *169*(1), 126–134. https://doi.org/https://doi.org/10.1016/j.cej.2011.02.066
41. Ortiz, D., Munoz, M., Nieto-Sandoval, J., Romera-Castillo, C., de Pedro, Z. M., Casas, J. A. (2022a). Insights into the degradation of microplastics by Fenton oxidation: From surface modification to mineralization. *Chemosphere*, *309*, 136809. https://doi.org/10.1016/j.chemosphere.2022.136809
42. Park, E. J., Park, B. C., Kim, Y. J., Canlier, A., Hwang, T. S. (2018). Elimination and substitution compete during amination of poly(vinyl chloride) with ehtylenediamine: XPS analysis and approach of active site index. *Macromolecular Research*, *26*(10), 913–923. https://doi.org/10.1007/s13233-018-6123-z
43. Piazza, V., Uheida, A., Gambardella, C., Garaventa, F., Faimali, M., Dutta, J. (2022). Ecosafety screening of photo-Fenton process for the degradation of microplastics in water. *Frontiers in Marine Science*, *8*. https://doi.org/10.3389/fmars.2021.791431
44. Shi, Y., Liu, P., Wu, X., Shi, H., Huang, H., Wang, H., Gao, S. (2021). Insight into chain scission and release profiles from photodegradation of polycarbonate microplastics. *Water Research*, *195*, 116980. https://doi.org/https://doi.org/10.1016/j.watres.2021.116980
45. Shihab, M. S., Ismail, H. H., Ibrahem, A. I. (2024). Adsorptive optimization of abamectin from aqueous solutions by immobilized *Eichhornia crassipes*. *Ecological Engineering & Environmental Technology*, *25*(10), 150–157. https://doi.org/10.12912/27197050/191412
46. Su, L., Liu, Z., He, J., Wu, Y., Wang, Q. (2024). The aging behavior of polyvinyl chloride microplastics by uv/sodium percarbonate oxidation: Efficiency and mechanism. *Water*, *16*(11), 1529. https://doi.org/10.3390/w16111529
47. Subramanian, S., Noh, J. S., Schwarz, J. A.

(1988). Determination of the point of zero charge of composite oxides. *Journal of Catalysis*, *114*(2), 433–439. https://doi.org/https://doi.org/10.1016/0021-9517(88)90046-2

48. Sulaiman, F., Alwared, A. (2022). Ability of response surface methodology to optimize photocatalytic degradation of amoxicillin from aqueous solutions using immobilized $TiO_2$/Sand. *Journal of Ecological Engineering*, *23*(5), 293–304. https://doi.org/10.12911/22998993/147318
49. Sun, Y., Yue, Q., Gao, B., Wang, B., Li, Q., Huang, L., Xu, X. (2012). Comparison of activated carbons from Arundo donax Linn with $H_4P_2O_7$ activation by conventional and microwave heating methods. *Chemical Engineering Journal*, *192*, 308–314. https://doi.org/https://doi.org/10.1016/j.cej.2012.04.007
50. Tofa, T. S., Kunjali, K. L., Paul, S., Dutta, J. (2019). Visible light photocatalytic degradation of microplastic residues with zinc oxide nanorods. *Environmental Chemistry Letters*, *17*(3), 1341–1346. https://doi.org/10.1007/s10311-019-00859-z
51. Wang, Z., Fang, C., Mallavarapu, M. (2015). Characterization of iron–polyphenol complex nanoparticles synthesized by Sage (*Salvia officinalis*) leaves. *Environmental Technology & Innovation*, *4*, 92–97. https://doi.org/https://doi.org/10.1016/j.eti.2015.05.004
52. Warrier, A. K., Kulkarni, B., Amrutha, K., Jayaram, D., Valsan, G., Agarwal, P. (2022). Seasonal variations in the abundance and distribution of microplastic particles in the surface waters of a Southern Indian Lake. *Chemosphere*, *300*, 134556. https://doi.org/https://doi.org/10.1016/j.chemosphere.2022.134556
53. Wu, S., Jin, T., Cheng, J., Zhou, H., Cheng, M. (2015). Air-assisted liquid liquid-microextraction for the analysis of fungicides from environmental water and juice samples. *Journal of Chromatographic Science*, *53*(6), 1007–1012. https://doi.org/10.1093/chromsci/bmu136